

Pump-Probe Photocurrent Measurements in Topological Insulators

Julia Radtke, Clark Travglini, Dong Yu

Abstract

Pump-probe photocurrent spectroscopy can be used to better understand the charge carriers in topological insulators. Pump-probe measurements were taken at both cold temperatures (80 K) and room temperature (293 K). At both temperatures, the effects of wavelength, pump power, and probe power were examined. It was found that at cold temperatures, there was a clear relationship between pump fluence and charge carrier relaxation time. Fluence did not seem to affect relaxation time at room temperature; however, more measurements could be taken to further examine this relationship.

Introduction

Topological insulators are quantum materials with many unusual properties making them an active area of condensed matter physics research [1]. One of the defining characteristics of a topological insulator is its inverted band structure, which is shown in Figure 1, caused by strong spin-orbit coupling. This unique band structure allows the material to have conductive surface states, which are protected from disorder and scattering, while the bulk of the material acts as an insulator. Understanding the behavior of the conductive surface states in topological insulators could have applications in spintronics, quantum computing, and other electronic devices.

One way to learn more about the conductive surface states in a topological insulator is to study the way the charge carriers behave when they are excited by light. If the electrons on the surface of the material absorb enough light energy, they can jump from the valence band to the conduction band resulting in a photocurrent that can be measured in the lab. One technique that can be used for this purpose is pump-probe spectroscopy. In pump-probe spectroscopy, two laser beams called the pump and probe interact with a sample. The pump beam sends out a pulse onto the sample which excites some of the charge carriers creating a photocurrent. After a short time delay, a second beam called the probe sends out an ultrafast pulse, and the photocurrent is measured. Pump-probe spectroscopy measurements can provide information about the excitation and relaxation time of the charge carriers, the types of charge carriers present, and the effects that different parameters have on measured photocurrent. Scanning photocurrent microscopy (SPCM) is another type of laser spectroscopy that can be used to map photocurrents throughout the surface of the device by scanning a laser beam across different slices of the material and measuring the generated photocurrent. The pump can be kept in a fixed location while the probe scans and measures photocurrent as a function of position. SPCM can provide information about how close the pump and probe must be to interact for

different time delays. Knowing this information can be used to infer the speed of the charge carriers.

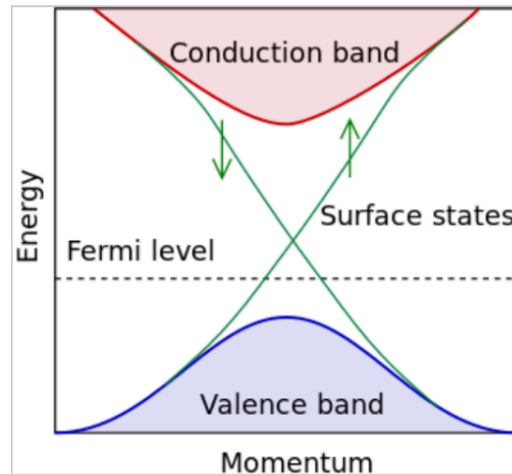


Figure 1. Valence band structure for a topological insulator [2]

Device Fabrication and Preparation

The topological materials used in this experiment were nanoribbons of Bi_2Se_3 doped with antimony to fill vacancies in the lattice. Nanoscale materials are ideal for studying the photocurrent behavior of the conductive surface states because of their high surface area to volume ratio. The topological nanomaterials were grown by chemical vapor deposition on a silicon substrate using Bi_2Se_3 and excess antimony and selenium as precursors. The nanoribbons were transferred onto a silicon wafer with a SiO_2 coating and gold electrodes. The transfer was done by scooping the nanomaterial from the substrate using a piece of cat hair and placing the material onto the wafer. The wafers were then spin-coated to protect the device. Microscope images of the wafers with the transferred material were taken using AmScope software and an optical microscope. To plan out how the material would be connected to the electrodes, device patterns were created using DesignCad software, and the gold contact connections were made using electron beam lithography. The devices' conductivities were measured to ensure that the surface states of the devices were conductive and that their contacts were ohmic. In some cases, a device that did not initially exhibit ohmic behavior could be made ohmic with voltage annealing, which can burn unwanted barriers within the device or contacts. The usable devices were then stored in a vacuum chamber to prevent the materials from being affected by moisture in the air until the spectroscopy part of the experiment.

Measurement

A schematic diagram of the optical table setup is shown in Figure 2. A MaiTai laser, which can produce light in the red and infrared range, was used as a beam source. A

beam splitter was used to separate the laser into two beams that could travel down two different paths. Mirrors were used to direct the beams down each path, and beam expanders were used to expand the beams. During the earlier measurements, a chopper, which was set to a frequency of 997 Hz, was used to break the beam into square waves so that the measured signal could be distinguished from background noise. During later measurements, the chopper was replaced with a photoelastic modulator since the chopper was too slow relative to the timescale of the measurements taken. A neutral-density filter was used to control the intensity of the light. For the low-temperature measurements, liquid nitrogen was used to cool the device.

Before taking the measurements, the laser was aligned and focused on the sample under an object lens. The location of the laser on the sample was chosen to be where a maximum signal was read since it was important to optimize the signal to background noise ratio to get the best measurements possible. The effects of multiple parameters were investigated during different trials including temperature, wavelength, and pump and probe fluence. The pump and probe fluences could be tuned using a filter, and the laser wavelength was set using a computer. The delay stage could be altered by changing the location of a crystal from which the probe beam was reflected, making the path length of the probe beam longer or shorter. Since the optical table had a floating setup, it was necessary to ensure that nothing touched or moved the table during a measurement to minimize unwanted noise signals. Once the optical table was set up, and the desired parameters were tuned and recorded, the measurement was taken using a computer. Both pump-probe spectroscopy and SPCM were performed. To measure the current, the gold electrodes on our device were connected to an ammeter to form a circuit. A diagram of this is shown below in Figure 3.

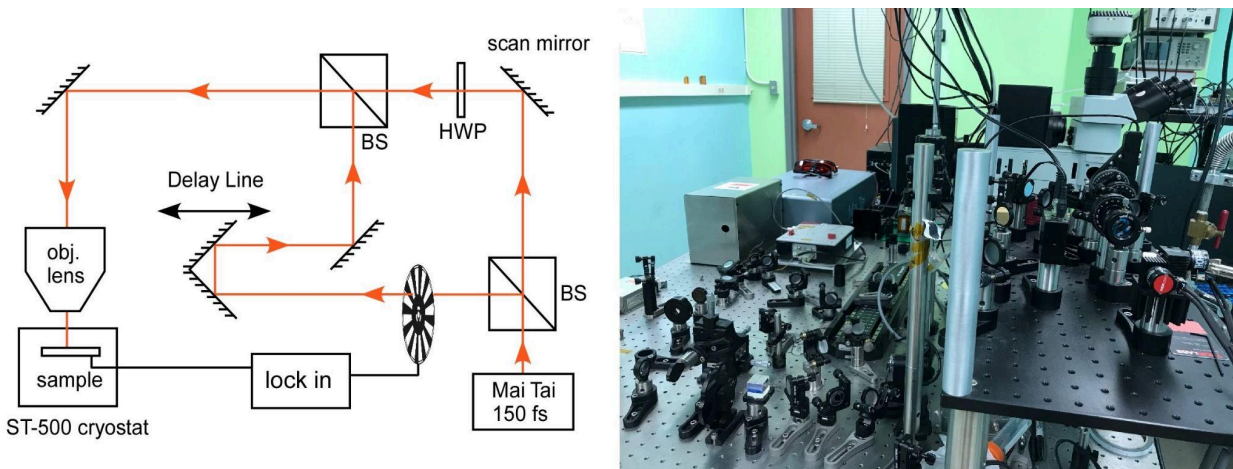


Figure 2. Pump-probe photocurrent spectroscopy setup

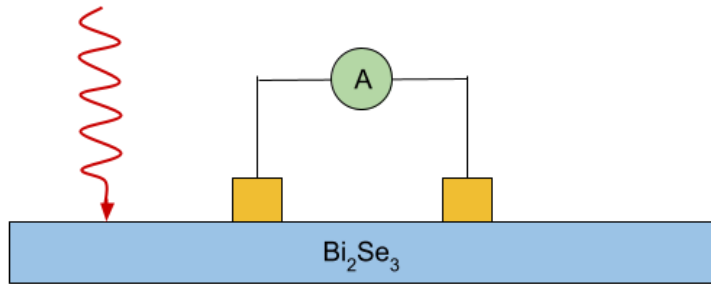


Figure 3. Device circuit diagram used for measurements

Data Processing and Analysis

The pump-probe measurements were uploaded and analyzed using Spyder, an analysis software using Python. A graph of the photocurrent vs. delay time was made showing the up, down, and averaged scans. A few of the trials did not produce useful plots because the peak signal was too weak to distinguish from the background noise present during the measurements; however, many of the plots showed a clear peak that could be further analyzed. Another plot was made of only the averaged photocurrent vs. delay time, and a curve was fit to the left and right sides of the peak. An example of this plot is shown in Figure 4. This curve fit was used to calculate the left and right relaxation times with error. The calculated left and right relaxation times with error bars were plotted as a function of probe fluence for four different room temperature trials in which all other parameters were held constant to investigate whether relaxation time had a fluence dependence at room temperature.

The SPCM data was also analyzed in Spyder. The t_0 delay vs. displacement of the probe from the pump was plotted, where t_0 is the delay in the time needed for the pump and probe to interact. Additionally, a photocurrent map of the material's surface was created by putting together data from scans through multiple different slices of the device. A sample photocurrent map is depicted in Figure 5. Finally, a plot showing photocurrent vs. delay lines at multiple positions was made, and t_0 for each position was calculated and marked on the plot as shown in Figure 6. The lines moving up represent the pump and probe getting farther apart.

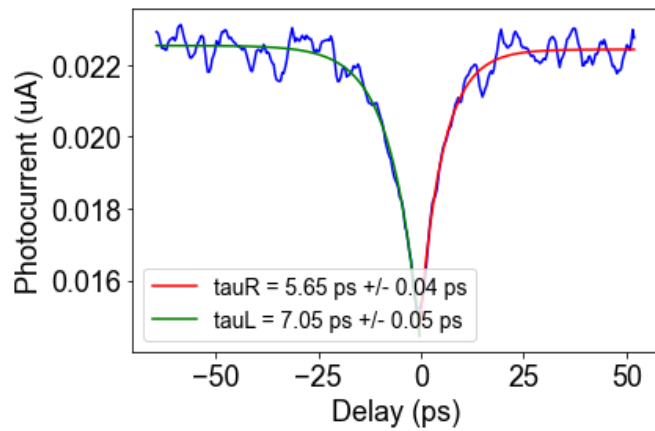


Figure 4. Photocurrent vs. Delay Time plot

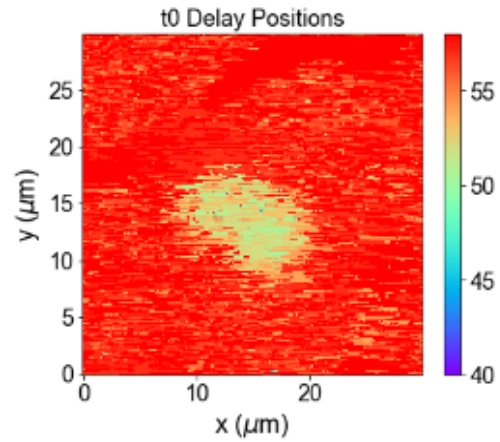


Figure 5. Photocurrent map

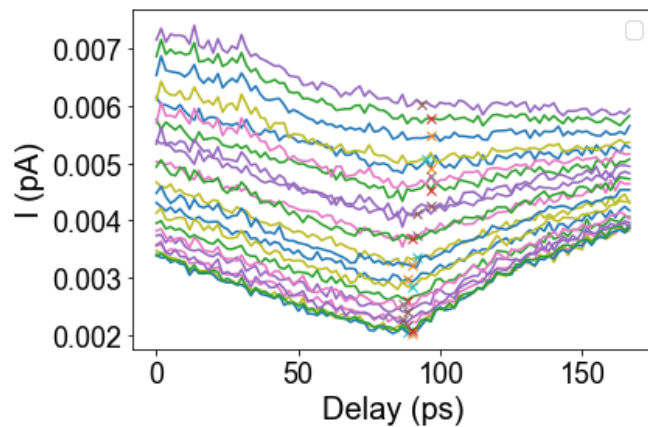


Figure 6. Photocurrent vs. Delay at different positions. The different traces represent measurements taken with different pump-probe displacement with photocurrent increasing as the pump and probe are moved farther apart.

Results and Discussion

For most of the pump-probe spectroscopy measurements, a reduction in photocurrent was observed. This photocurrent reduction was expected because when some electrons have already been excited into the conduction band by the pump, there are fewer electrons left in the valence band for the probe to excite. A diagram of this process is shown in Figure 7.

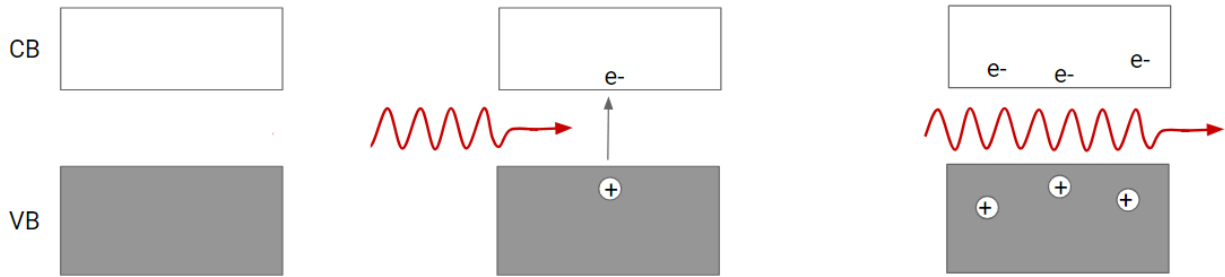


Figure 7. Photocurrent reduction process.

When the laser was focused near the device's electrodes, there could sometimes be an enhancement in photocurrent instead of a reduction. This enhancement may be attributed to band bending near the electrodes. Wavelength had no clear wavelength dependence at room temperature, but it is difficult to judge with certainty whether or not relaxation time is wavelength-dependent since some of the curve fittings could have been off due to background noise or weak signals. There were many noticeable differences between the data collected at low and high temperatures. The low-temperature measurements showed strong fluence dependence with a longer carrier lifetime at higher fluences. Faster carrier recombination at high temperatures is expected due to the increased number of phonons that charge carriers can interact with. At cold temperatures, it was possible to greatly reduce the photocurrent, almost completely turning off the measured signal. Example plots showing photocurrent measurements for high and low fluences at 80 Kelvin are shown below in Figure 8.

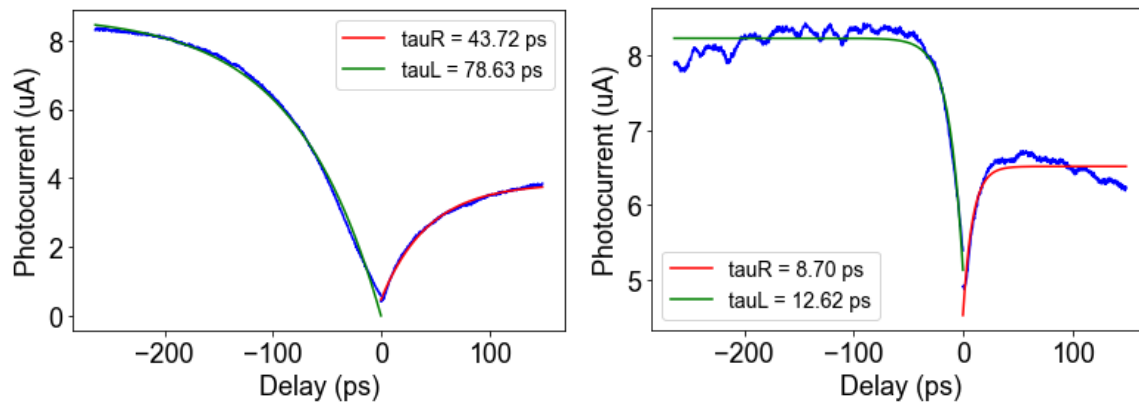


Figure 8. Photocurrent measurement plots for 80 K (left) and 293 K (right)

To compare how pump fluence affects photocurrent at high versus low temperatures, two plots were made, showing the left and right relaxation times as a function of fluence at 293 Kelvin and the left and right relaxation times as a function of fluence at 80 Kelvin. These plots are shown below in Figure 9. For the room temperature measurements, the relaxation times were very short. The data was scattered and relaxation

time did not appear to have a strong dependence on fluence. For the cold temperature measurements, however, the relaxation time was longer and did show fluence dependence. At room temperature, the material is believed to be hot carrier dominated, and the relaxation process for charge carriers involves electrons recombining with holes.

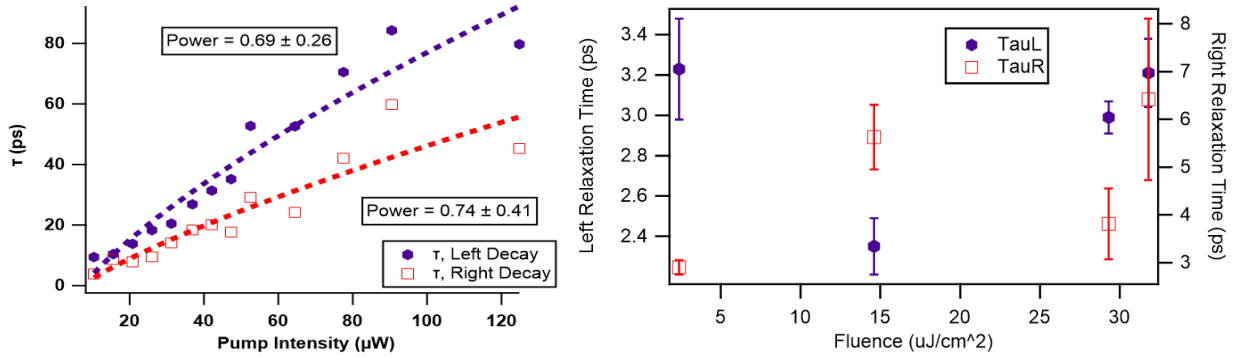


Figure 9. Relaxation time vs pump intensity at 80 K with a power function fit to the data (left) vs relaxation time vs pump intensity at 293 K (right)

Some of the t_0 maps turned out much clearer than others. When the 1.8 μW probe was used, higher pump powers tended to give stronger signals, but when a 5.0 μW probe was used, some of the lower probe powers gave very clear signals. The t_0 delay vs. pump-probe displacement data can be used to estimate the velocity of the charge carriers. If the time difference between the pump and probe pulses as well as how close the pump and probe have to be to interact are known, the average velocity of the charge carriers can be found by dividing the displacement by the time difference. Since the signals got weaker as the pump and probe were moved farther apart, the t_0 values calculated from the photocurrent delay line for greater pump-probe displacements could be inaccurate.

At cold temperatures, the measured current for higher fluences was found to drop much more and to decay more slowly than for low fluences at the same temperature. This is most likely because the electrons and holes can recombine before reaching the electrodes at lower fluences. Another possible explanation is that charge carriers may get trapped at the interface between the contacts and Bi_2Se_3 . After getting trapped, the carriers would take around 100 ps to be released.

In addition to measuring photocurrent to understand how the conductive surface states behave in a topological insulator, reflectance measurements, which involve shining a light onto a sample and measuring the fraction of light that is reflected, is another way to examine the surface state behavior. Even though it was expected that photocurrent and reflectance measurements would exhibit similar dependences on fluence, it was found that the fluence dependence for photocurrent was opposite to reflectance measurements. Increasing fluence in this experiment resulted in a slower photocurrent decay. One possible explanation for this is screening. The electrons and holes could form an exciton

condensate in which electrons and holes pair up such that they have an integer combined spin and exhibit superfluid behavior [3]. The rate at which electrons recombine with holes would then depend on the effective Coulombic attraction between the electrons and holes. If fluence is high, there is a greater electron density because other electrons in the material can surround the hole making the electron less attracted to the hole and slowing down the rate of recombination.

Conclusion and Next Steps

In this lab, multiple pump-probe spectroscopy and SPCM measurements were taken at room temperature and cold temperatures. Although the data collected in this lab helped provide some insights such as the relaxation times of charge carriers under different conditions, how long it takes the pump and probe to interact depending on their displacement from each other, and photocurrent maps for different pump-probe delays, some of the data is not clear enough to draw conclusions from. More measurements could be taken at room temperature to examine fluence dependence since the data appears scattered, and there are not enough data points to establish with confidence whether they follow a pattern. It would also be interesting to look for evidence to support or challenge the idea that shielding slowing down the electron-hole recombination is the reason the measurements taken in this experiment have a different fluence dependence behavior than measurements from the reflectance lab.

Sources

[1] Sun, D., Aivazian, G., Jones, A. M., Ross, J. S., Yao, W., Cobden, D., & Xu, X. (2012). Ultrafast hot-carrier-dominated photocurrent in graphene. *Nature Nanotechnology*, 7(2), 114–118. <https://doi.org/10.1038/nnano.2011.243>

[2] *Topological insulator*. (n.d.). Assignment Point.
<https://assignmentpoint.com/topological-insulator/>

[3] Hou, Y., Wang, R., Xiao, R., McClintock, L., Travaglini, H. C., Francia, J. P., Fetsch, H., Erten, O., Savrasov, S. Y., Wang, B., Rossi, A., Vishik, I., Rotenberg, E., & Yu, D. (2019). Millimetre-long transport of photogenerated carriers in topological insulators. *Nature Communications*, 10(1).
<https://doi.org/10.1038/s41467-019-13711-3>